

Supporting Information for

**Enhanced lubrication and photothermal conversion via  
dynamically reversible supramolecular oil gels filled with  
MXene@mGLM composites**

*Yuhong Cui<sup>a</sup>, Tiantian Wang<sup>a</sup>, Guangkai Jin<sup>a</sup>, Shiyuan Wang<sup>a</sup>, Shujuan Liu<sup>a</sup>, Qian*

*Ye<sup>a,\*</sup>, Feng Zhou<sup>a,b</sup>, Weimin Liu<sup>a,b</sup>*

<sup>a</sup>State Key Laboratory of Solidification Processing, Center of Advanced Lubrication and Seal Materials, School of Materials Science and Engineering, Northwestern Polytechnical University, Xi'an, 710072, P. R. China.

<sup>b</sup>State Key Laboratory of Solid Lubrication, Lanzhou Institute of Chemical Physics, Chinese Academy of Sciences, Lanzhou, 730000, P. R. China.

\*Corresponding author: [yeqian213@nwpu.edu.cn](mailto:yeqian213@nwpu.edu.cn) (Qian Ye)

## **Materials**

Gallium-based liquid metal (GLM, Ga<sub>80</sub>In<sub>20</sub>) was obtained from Shenyang Jiabei Trading Co., Ltd. Acetone, hydrochloric acid (HCl) and Tannic acid (TA) were purchased from Sinopharm Chemical Reagent Beijing Co., Ltd. Lithium fluoride (LiF) was obtained from Energy Chemical. MAX (Ti<sub>3</sub>AlC<sub>2</sub>) was purchased from Jinzhou Haixin Metal Materials Co., Ltd. 12-Hydroxyoctadecanoic Acid (12-HSA) came from Shanghai Aladdin Biochemical Technology Co., Ltd.

## **Characterization**

Transmission electron microscope (TEM, Talos F200X) and scanning electron microscope (SEM, Tescan Clara GMH) was used to analyze the morphology and microstructure. The chemical states and crystal structure of the samples were analyzed by X-ray photoelectron spectroscopy (XPS, PHI 5000 VersaProbe III) and X-ray diffraction (XRD, D8 ADVANCE). The full XPS spectrum ranged from 0 to 1100 eV with a step size of 1 eV. For a narrow spectrum, each element was scanned 5 times and cycled 2 times, with a step size of 0.125 eV. XRD diffraction angle test range was 5°~90°, scanning speed was 5°/min. Using Malvern Zetasizer Nano zeta potential analyzer to detect the alteration of surface charge. Thermogravimetric analysis (TGA, STA 449F3) was carried out under Ar atmosphere (35-700 °C, 10 °C/min). The Raman spectra were measured by laser confocal Raman microspectrometer (Renishaw inVia Reflex). Using Bruker Tensor II infrared spectrometer to record fourier transform infrared (FTIR) spectrum. Differential Scanning Calorimeter (DSC 214) and commercial rheometer HAAKE MARS III. were used to measure the

rheological characteristics of the gel. Used an infrared thermal imager (FLIR, E8-XT, USA) to record the changes in the surface temperature of the gel.

The tribological performance were tested by SRV-5 tribometer with a ball-on-disk mode. The ball ( $\varnothing$  10 mm,  $60 \pm 2$  HRC, mean roughness 20 nm) and disk ( $\varnothing$  24 mm  $\times$  7.9 mm,  $62 \pm 2$  HRC) were made of AISI 52100 steel. The wear depth, wear volume and topography of the worn surface were calculated by a three-dimensional (3D) surface profiler (Bruker, NPFLEX). Test conditions: load 150 N, frequency 25 Hz, temperature 50 °C and stroke 1 mm. Frequency conversion test: under the condition of amplitude of 1 mm, temperature of 50 °C and load of 150 N. The frequency increased from 5 Hz to 45 Hz, increasing by 5 Hz every 5 minutes. Variable temperature test: under the condition of amplitude of 1 mm, frequency of 25 Hz and load of 150 N. The temperature rose from 40 °C to 120 °C, increasing by 10 °C every 5 minutes.

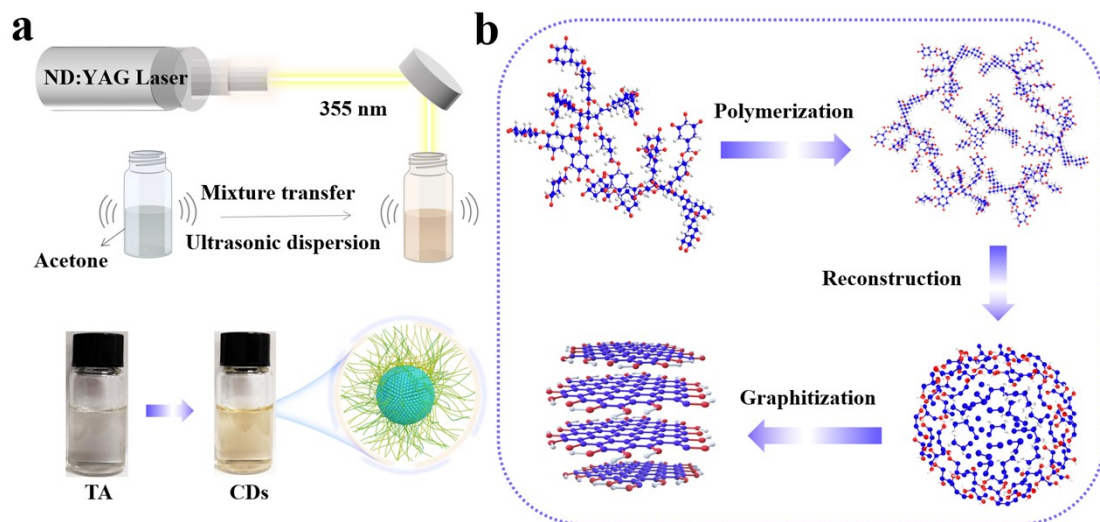


Fig. S1 Schematic illustration of CDs generated by pulsed laser treatment.

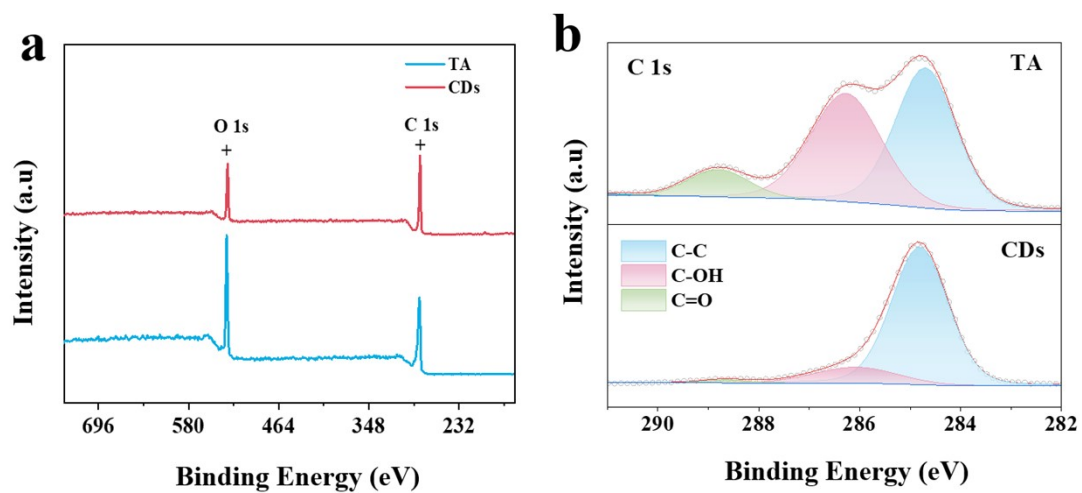


Fig. S2 (a) XPS full spectrum and (b) XPS high spectrum of C 1s of TA and CDs.

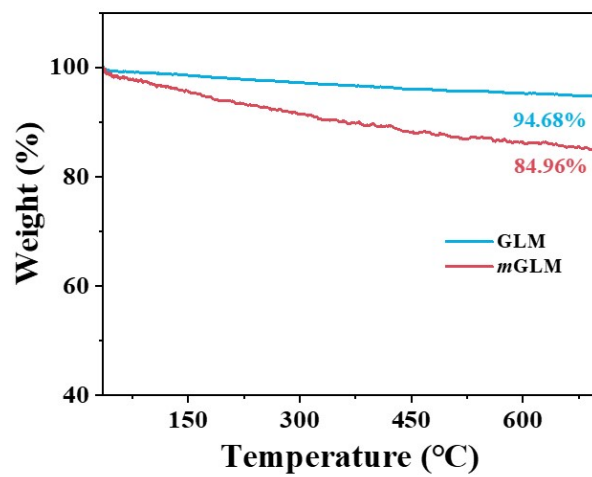


Fig. S3 TGA curves of GLM and *m*GLM.

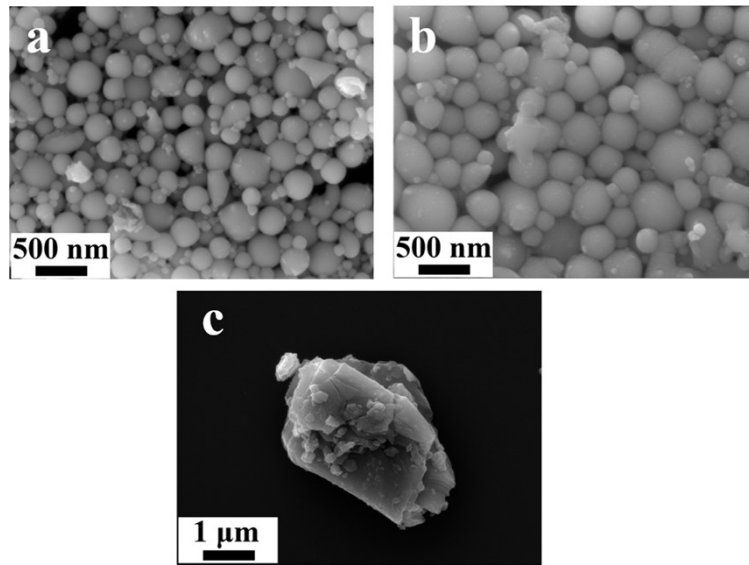


Fig. S4 SEM images of (a) GLM, (b) *m*GLM and (c)  $\text{Ti}_3\text{AlC}_2$  MAX.

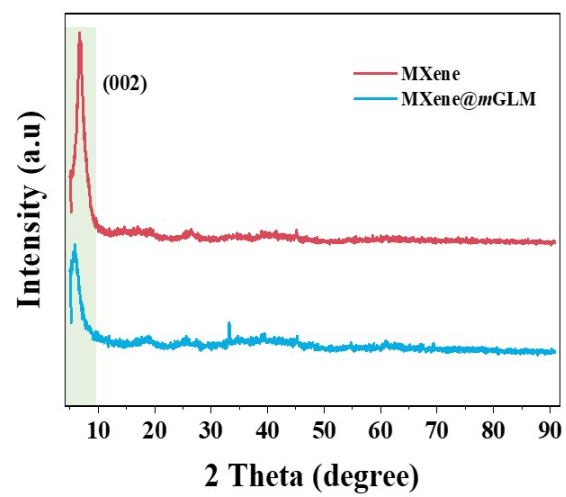


Fig. S5 XRD pattern of MXene and MXene@mGLM.



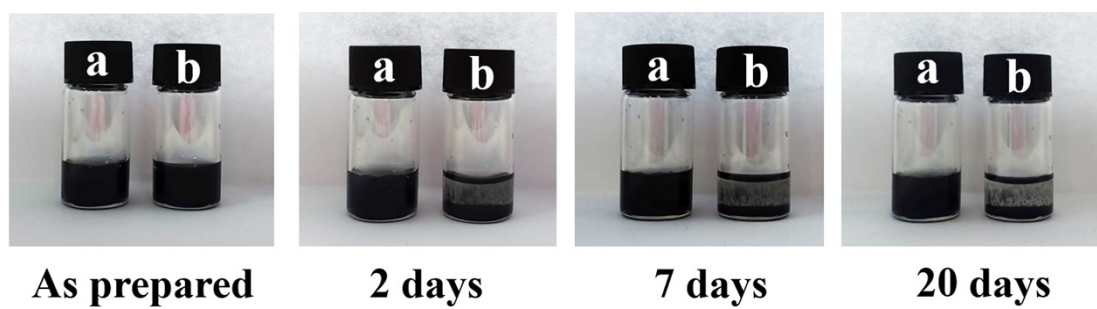


Fig. S6 Comparison of dispersion stability between (a) gel state and (b) solution of MXene@mGLM.

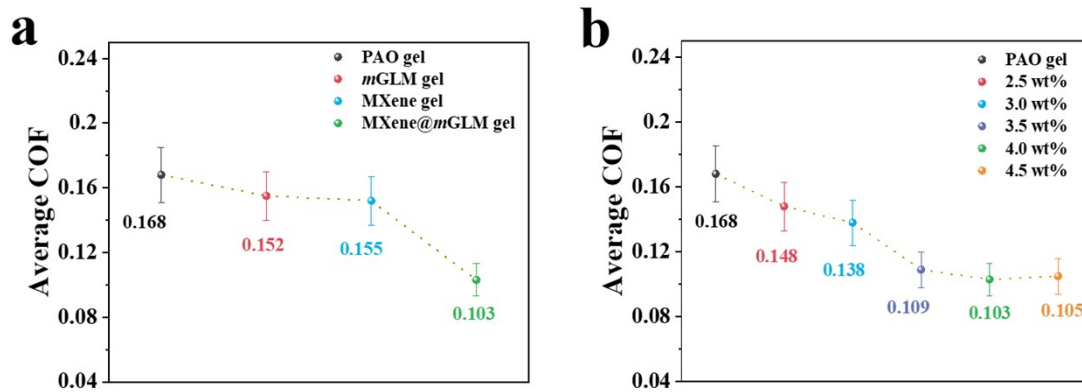


Fig. S7 (a) Average COF of PAO gel, *m*GLM gel, MXene gel and MXene@*m*GLM gel. (b) Average COF of MXene@*m*GLM gel with varying addition concentrations.

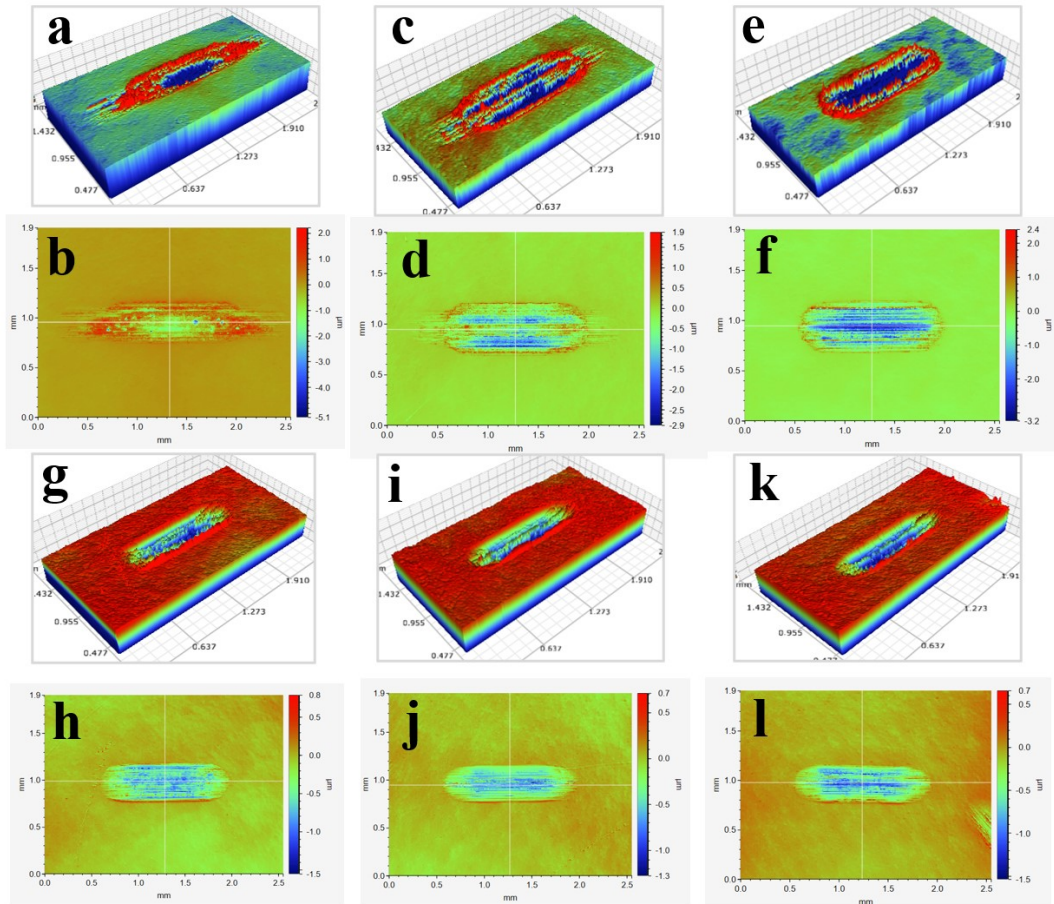


Fig. S8 The 3D contour images of steel disk scratches lubricated by MXene@mGLM gel with varying addition concentration: (a, b) 0 wt%, (c, d) 2.5 wt%, (e, f) 3.0 wt%, (g, h) 3.5 wt%, (I, j) 4.0 wt% and (k, l) 4.5 wt%.

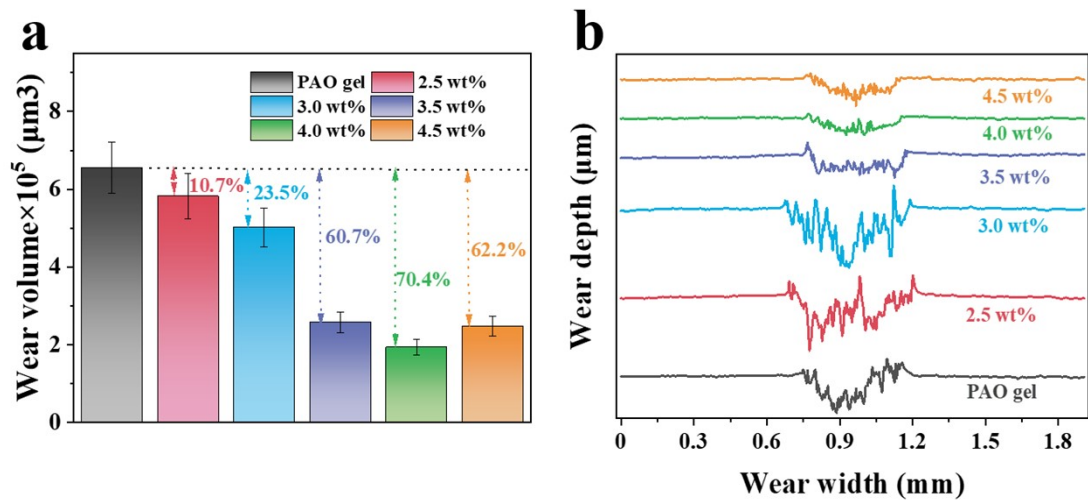


Fig. S9 (a) Wear volume and (b) Wear depth of steel disk scratches lubricated by MXene@mGLM gel with varying addition concentration.

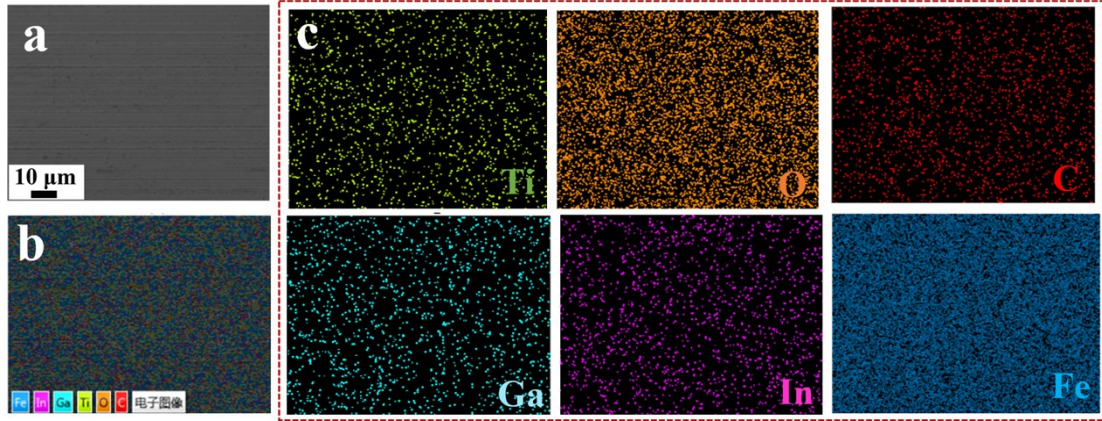


Fig. S10. (a b) SEM and (c) element mapping images of worn surface lubricated by MXene@mGLM gel.